

# Deep Near Infrared Photometry of New Galactic Globular Clusters <sup>★</sup>

Valentin D. Ivanov<sup>1</sup>, Jordanka Borissova<sup>2</sup>, and Leonardo Vanzi<sup>3</sup>

<sup>1</sup> Steward Observatory, The University of Arizona, Tucson, AZ 85721, U.S.A., vdivanov@as.arizona.edu

<sup>2</sup> Institute of Astronomy, Bulgarian Academy of Sciences and Isaac Newton Institute of Chile, Bulgarian Branch, 72 Tsarigradsko chausseè, 1784 Sofia, Bulgaria, jura@haemimont.bg

<sup>3</sup> European Southern Observatory (ESO), Alonso de Cordova 3107, Santiago - Chile

Received 24 08 2000 / Accepted 13 09 2000

**Abstract.** We present a preliminary report on the first deep infrared photometry of 2MASS GC01 and 2MASS GC02 (GC01 and GC02 hereafter) - new Galactic globular cluster (GC) candidates, discovered by the 2MASS. They both appear to be genuine disk GCs though highly obscured. The location of the two GCs suggests that they are metal rich -  $[\text{Fe}/\text{H}] \sim -0.5$ . We estimated their distance and reddening using the  $K_s$  - band brightness of the red giant branch (RGB) bump, and  $J - K_s$  color of the RGB at  $M_K = -3$  mag:  $D = 3.1 \pm 0.5, 3.9 \pm 0.6$  kpc, and  $A_V = 20.9 \pm 0.7, 17.2 \pm 1.2$  mag, for GC01 and GC02 respectively. Variation in the metal abundance can change our results within 30 - 35%.

**Key words:** The Galaxy: globular clusters: general - The Galaxy: abundances - The Galaxy: globular clusters: individual: 2MASS GC01 - The Galaxy: globular clusters: individual: 2MASS GC02 - Stars: Hertzsprung-Russel and C-M diagrams - Stars: distances

## 1. Introduction

The known Galactic globular clusters (GC) - less than 150 (Harris 1996) - were discovered mostly through optical searches, that are obviously biased against highly obscured GCs. Since the Galaxy is estimated to have  $160 \pm 20$  GCs (Harris 1991), a certain number of them may still be hidden behind the Galactic disk. The Two Micron All Sky Survey (2MASS) offers an opportunity to carry a search for the missing GCs, and recently Hurt et al. (1999, 2000) reported a serendipitous discovery of two new GCs: 2MASS GC01 and 2MASS GC02 (GC01 and GC02 hereafter). Their estimates suggest  $A_V = 18 - 20$  mag, rendering these clusters unobservable in the optical wavebands. A summary of the available data for the new clusters is given in Table 1 (Hurt et al. 2000).

Send offprint requests to: Valentin D. Ivanov

<sup>★</sup> Based on data obtained at the ESO-NTT in La Silla, Chile.

**Table 1.** Basic cluster data

Name	R.A. Dec (2000)	Diameter (arcmin)	Core Magn $K_s$
GC01	18:08:21.81 -19:49:47	$3.3 \pm 0.2$	$7.2 \pm 0.4$
GC02	18:09:36.50 -20:46:44	$1.9 \pm 0.2$	$5.5 \pm 0.2$

Situated in the general direction of the Galactic center, the new GCs are probably members of the disc system of GCs, which provides a valuable test case for understanding of the evolution of metal rich stars.

Deep imaging in the near-infrared (NIR) is the only feasible way to study the new clusters. Glass & Feast (1973), and Davidge & Simons (1991), among others, have demonstrated the usefulness of the NIR photometry of GCs for reddening and distance determinations. Recently, Kuchinski, Frogel & Terndrup (1995), Ferraro et al. (2000) and Ivanov et al. (2000) demonstrated photometric techniques to estimate the metal abundance  $[\text{Fe}/\text{H}]$  of GCs using the slope of the red giant branch (RGB) in the  $K_s$  vs.  $J - K_s$  diagram, with accuracy of 0.1 - 0.15 dex.

The development of the NIR methods and the extremely high reddening towards GC01 and GC02 prompted us to carry out the first deep NIR  $JK_s$  photometry of the two clusters. We present here preliminary estimates on their distance and reddening. A more detailed analysis and additional data will be reported in a subsequent paper.

## 2. Observations and Data Reduction

The clusters GC01 and GC02 were observed at the ESO-NTT with SOFI in different occasions during July 2000. We used the Large-Field setup with a plate scale of  $0.292$  arcsec pixel<sup>-1</sup>, and a field of view  $5 \times 5$  arcmin that allows to cover the entire clusters. The total integration time was 15, 10 and 15 minutes for GC01, and 25, 15 and 15 for GC02, respectively in J, H and  $K_s$ . These observations were taken under non-photometric conditions. We

**Fig. 1.** Near infrared 3-color composite image of GC01. The J, H, and  $K_s$  bands are mapped onto blue, green and red, respectively. The image is 4.98 arcmin on the side. North is up, and East is to the left.

also acquired 1 minute calibration images under photometric conditions. The seeing ranged between 0.6 and 0.8 arcsec. A 3-color composites of the two clusters are shown in Figs. 1 and 2.

The observational strategy consisted in alternating images on the objects and on the nearby sky (ON-OFF technique) to account for the sky background variations. Due to the high brightness of a few stars in the field, the images were taken with a short integration time, typically 1.2 sec, and were coadded at each position. The total integration time at each position was 60 sec. We introduced a random shift of  $\sim 5 - 10$  arcsec between each object frame to improve the bad pixel and cosmic ray correction. The sky frames were taken at  $\sim 10$  arcmin from the clusters.

The data reduction included flat-fielding, and sky subtraction using IRAF<sup>1</sup>. The images were shifted to a common position with fractional shifts and linear interpolation, and median combined together to produce the final image. The photometric calibration was performed using 2MASS stars (40 – 60, depending on the band) in the field of GC01 as photometric standards, with typical r.m.s. = 0.05 – 0.07 mag. The stellar photometry of the final combined images was carried out using DAOPHOT II (Stetson1993). In this letter we consider only stars with DAOPHOT errors less than 0.15 mag. The median averaged  $1\sigma$  errors over 1 mag bins are shown in Fig. 3. There is also an additional observational error of  $\sim 0.01$  mag due to the sky background variations. The effects of the crowd-

**Fig. 2.** Near infrared 3-color composite image of GC02. The size and orientation are the same as in Fig. 1.

ing will be studied in the main paper by adding artificial stars in the field, and than measuring their brightness.

The brightest stars ( $K_s \leq 10$  mag) in our photometry are affected by the non-linearity of the array. For the purposes of this letter we will use only the fainter stars. A more comprehensive analysis and a non-linearity correction will be presented in a future paper.

### 3. Analysis

The J –  $K_s$  vs.  $K_s$  color-magnitude diagrams (CMD) of the two clusters are shown in Fig. 3. The most prominent features are the RGBs at  $J - K_s \sim 3 - 4.5$  mag, and the main sequences (MS) of the field stars at  $J - K_s < 2$  mag. They are both widened by the photometric uncertainties, and in the case of MS's - by distance and reddening variations.

To eliminate the field contamination at least partially, we constructed the same CMDs for stars within 30 and 20 arcsec from the cluster centers, respectively for GC01 and GC02 (Fig. 4). Although some blue disk stars are still present, the plots are dominated by cluster members. The red clumps are visible, at  $K_s = 13.5 - 14.5$  mag. Since the RGB bump stars are not affected by the non-linearity, we can use them to deduce the cluster distances.

The position of the RGB on the J –  $K_s$  vs.  $K_s$  CMD contains information about the metal abundance of the clusters. Fiducial lines, that represent slopes of RGBs for  $[\text{Fe}/\text{H}] = -0.5, -1, \text{ and } -2$ , according to the calibration of Ivanov et al. (2000), are shown in Fig. 4. Although the statistics is small, the plot is consistent with GC02 being metal rich. Given the location of the GCs in the Galaxy, we will assume throughout the paper that both GC01 and GC02 have metallicity of  $[\text{Fe}/\text{H}] = -0.5$ .

The RGB bump is more obvious on the  $K_s$  – band luminosity function (LF) plots (Fig. 5). Again, we selected

<sup>1</sup> IRAF is distributed by the National Optical Astronomy Observatories, which are operated by the Association of Universities for Research in Astronomy, Inc., under cooperative agreement with the National Science Foundation.

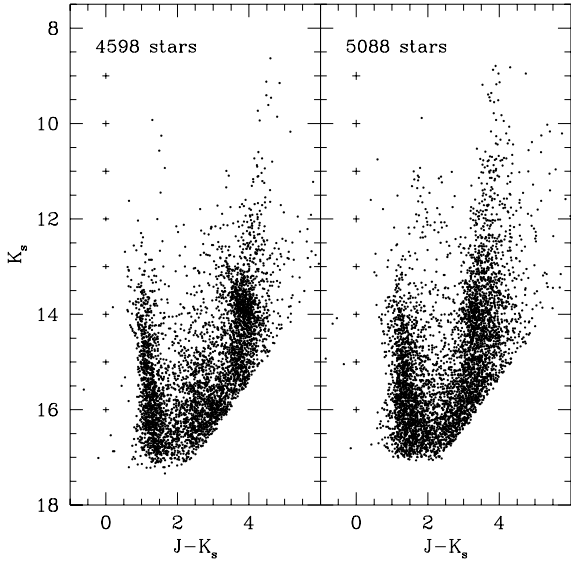


**Fig. 3.** The  $J - K_s$  vs.  $K_s$  color-magnitude diagrams of all stars in the fields of GC01 (left panel) and GC02 (right panel). The numbers of stars are indicated. DAOPHOT errors, (median averaged over 1 mag bins) are shown on the left.

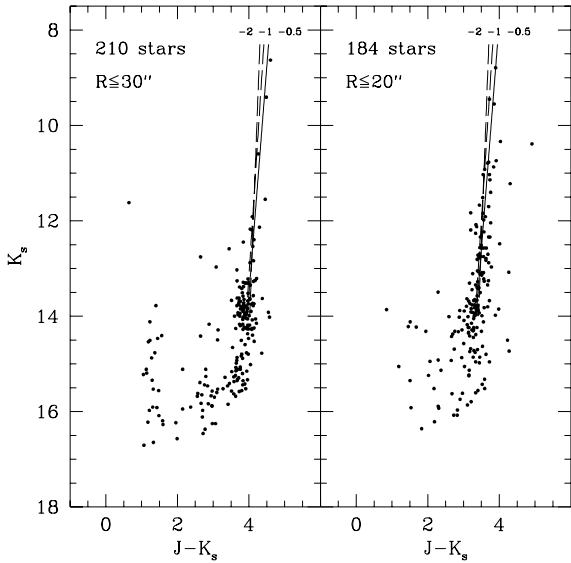


**Fig. 4.** The  $J - K_s$  vs.  $K_s$  color-magnitude diagrams of the central  $30''$  and  $20''$  of GC01 (left panel) and GC02 (right panel), respectively. The numbers of stars are indicated. Fiducial lines, corresponding to the RGB slopes for  $[\text{Fe}/\text{H}] = -2, -1, \text{ and } -0.5$  (from left to right) are shown.

only stars near the cluster centers (top panels), to minimize the effect of the field star contamination. For comparison purpose we also constructed the LFs for identical areas (second panels), well outside the cluster limits of ( $R_{\text{cl}} = 99 \pm 6$  and  $57 \pm 6$  arcsec for GC01 and GC02,

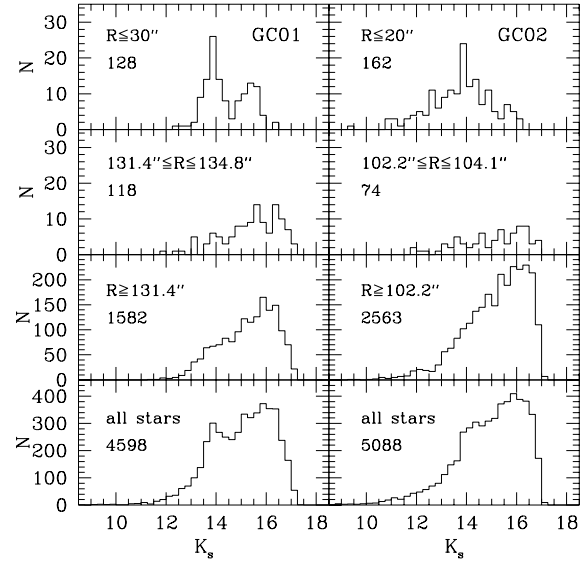


**Fig. 5.** Luminosity functions. GC01 is on the left hand side, and GC02 is on the right hand side. The top panels show the LFs in the central regions. The second panels show the LFs for regions with the same areas but outside of the cluster limits. The third panels show the LFs for all non-cluster stars, and the bottom panels show the LFs for the entire fields. The limits of the selected regions in terms of distance from the cluster centers  $R$ , and the number of stars, included in each LF are indicated on each panel.

Table 1). Although the field star numbers are large, they are dominated by the faintest stars, which are underrepresented in the cluster LFs. The severe crowding in the clusters leads to shallower cut-offs in the cluster LFs. At the positions of the RGB bumps the field stars account for only about 15% of the stars, and there is no trace of peaks. For completeness we plot the LFs of all non-cluster stars (third panels), and they also do not show detectable peaks at the position of the RGB bumps. Such traces are present in the LFs of the entire fields (bottom panels).

The first step in our analysis was to estimate accurately the position of the bump. Following the example of Alves (2000) we fitted Gaussian to the  $K_s$  - band LFs in the regions of the bumps, obtaining  $K_s = 13.86 \pm 0.30$  and  $K_s = 13.99 \pm 0.25$  mag, respectively for GC01 and GC02. The intrinsic spread of the stellar luminosities in the RGB bump accounts for the large uncertainties, in comparison with the photometric errors.

Next, we applied the calibration of the absolute  $K$  - band magnitude of the RGB bump  $M_K^b$  as a function of the cluster metallicity, by Ferraro et al. (2000). They used the metallicity scale of Carretta & Gratton (1997). Although their  $K$  filter is different from our  $K_s$  filter, a comparison between the  $K$  and  $K_s$  measurements of red stars in Persson et al. (1998) yields differences of only  $0.01 - 0.02$  mag,

negligible for the purpose of this analysis. Henceforth we consider K and  $K_s$  magnitudes equivalent.

The RGB bump brightness is rather sensitive to the metal abundance - according to Ferraro et al. (2000) it shifts from  $M_K^b = -0.92$  to  $M_K^b = -1.56$  for a metallicity change from  $[Fe/H] = -0.5$  to  $-1$ . We calculated  $(m - M)_0 + A_K = 14.78 \pm 0.35$  and  $14.91 \pm 0.31$  mag, respectively for GC01 and GC02.

To determine the reddening corrected distance moduli we used the color of the RGB. Ferraro et al. (2000) calibrated the RGB  $J - K$  color at a given  $M_K$  as a function of the metal content. Their faintest RGB level was  $M_K = -3$  mag. Once we knew the brightness of the RGB bump, we could find the  $M_K = -3$  mag level on our CMD, and calculated the  $(J - K)_{M_K=-3}$  color. We averaged the color of the stars over  $\pm 0.5$  mag interval, to ensure sufficient statistics. We estimated  $(J - K_s)_{M_K=-3} = 4.13 \pm 0.11$  and  $3.51 \pm 0.18$  mag for GC01 and GC02, respectively. The predicted intrinsic RGB color for  $[Fe/H] = -0.5$  was  $(J - K)_{0, M_K=-3} = 0.58 \pm 0.02$  mag, and the color excesses were  $E(J - K_s) = 3.55 \pm 0.22$  and  $2.93 \pm 0.18$  mag for GC01 and GC02. We used the reddening curve of Rieke & Lebofski (1985) to calculate the extinction:  $A_V = 20.88 \pm 0.65$  and  $17.24 \pm 1.23$ ,  $A_K = 2.34 \pm 0.07$  and  $1.93 \pm 0.14$  mag for GC01 and GC02. Finally, we obtained the reddening corrected distance moduli  $(m - M)_0 = 12.44 \pm 0.36$  and  $12.98 \pm 0.41$  mag, and distances  $D = 3.1 \pm 0.5$  and  $3.9 \pm 0.6$  kpc for GC01 and GC02, respectively. We performed the same estimates (Table 2) for  $[Fe/H] = -1$  and  $-2$ , although the latter seems unlikely, given the cluster location.

#### 4. Conclusions

We carried out the first deep NIR photometry of GC01 and GC02 - new Galactic GCs, discovered by the 2MASS. The data suggest that they are metal rich GCs, consistent with their location in the disk. We detected the RGBs and the RGB bumps and estimated their distance and reddening using the brightness of RGB bumps and the color of the RGB. We found  $D = 3.1 \pm 0.5$ ,  $3.9 \pm 0.6$  kpc, and  $A_V = 20.9 \pm 0.7$ ,  $17.2 \pm 1.2$ , for GC01 and GC02 respectively. Here, we assumed  $[Fe/H] = -0.5$ , typical for disk clusters, but a different metal abundance could change our results within 30 - 35%.

Our data suggest extinction similar to the  $A_V = 20 \pm 2$  and  $18 \pm 2$  mag for GC01 and GC02, obtained by Hurt et al. (2000). A better knowledge of the metal abundance is crucial for an accurate distance and reddening determination with this technique. We will report a more sophisticated Monte-Carlo foreground removal method, metallicity estimates, and deeper CMDs and color-color diagrams in a subsequent paper.

The authors are grateful to the referee Dr. R. Hurt for the helpful comments.

**Table 2.** Reddening and distance estimates.  $1\sigma$  errors are given in brackets. See Sect. 3 for details.

Parameter	GC01	GC02
$m_K^b$	13.86(0.30)	13.99(0.25)
$[Fe/H]$	-0.5	
$M_K^b$	-0.92(0.19)	
$(m - M)_0 + A_K$	14.78(0.35)	14.91(0.31)
$(J - K)_{M_K=-3}$	4.13(0.11)	3.51(0.18)
$(J - K)_0$	0.58(0.02)	
$E(J - K)$	3.55(0.22)	2.93(0.18)
$A_V$	20.88(0.65)	17.24(1.23)
$A_K$	2.34(0.07)	1.93(0.14)
$(m - M)_0$	12.44(0.36)	12.98(0.41)
$D(\text{kpc})$	3.1(0.5)	3.9(0.6)
$[Fe/H]$	-1.0	
$M_K^b$	-1.56(0.27)	
$(m - M)_0 + A_K$	15.42(0.40)	15.55(0.37)
$(J - K)_{M_K=-3}$	4.08(0.13)	3.50(0.14)
$(J - K)_0$	0.69(0.01)	
$E(J - K)$	3.39(0.13)	2.81(0.14)
$A_V$	19.94(0.76)	16.53(0.82)
$A_K$	2.23(0.09)	1.85(0.14)
$(m - M)_0$	13.19(0.41)	13.70(0.38)
$D(\text{kpc})$	4.3(0.8)	5.5(1.0)
$[Fe/H]$	-2.0	
$M_K^b$	-2.22(0.40)	
$(m - M)_0 + A_K$	13.08(0.50)	12.21(0.47)
$(J - K)_{M_K=-3}$	3.94(0.16)	2.70(0.16)
$(J - K)_0$	0.75(0.01)	
$E(J - K)$	3.19(0.16)	2.70(0.16)
$A_V$	18.76(0.94)	15.88(0.94)
$A_K$	2.10(0.11)	1.78(0.11)
$(m - M)_0$	13.98(0.51)	14.43(0.48)
$D(\text{kpc})$	6.3(1.5)	7.7(1.7)

#### References

- Alves, D.R., 2000, preprint (astro-ph/0003329)  
Carretta, E., Gratton, R., 1997, A&AS, 121, 95  
Davidge, T.J., Simons, D.A., 1991, AJ, 101, 1720  
Ferraro, F.R., Montegriffo, P., Origlia, L., Fusi Pecci, F., 2000, AJ, 119, 1282  
Glass, I.S., Feast, M.W., 1973, MNRAS, 163, 245  
Harris, W., 1991, ARA&A, 29, 543  
Harris, W., 1996, AJ, 112, 1487  
Hurt, R.L., Jarrett, T., Cutri, R., Skrutskie, M., Schneider, S., van Driel, W., 1999, AAS, 194.0711  
Hurt, R.L., Jarrett, T.H., Kirkpatrick, J.D., Cutri, R.M., Schneider, S.E., Skrutskie, M., 2000, preprint (astro-ph/0006262)  
Ivanov, V.D., Borissova, J., Alonso-Herrero, A., Russeva, T., 2000, AJ, 119, 2274  
Kuchinski, L.E., Frogel, J.A., Terndrup D.M., 1995, AJ, 109, 1131  
Persson, S.E., Murphy, D.C., Krzeminski, W., Roth, M., Rieke, M.J., 1998, AJ, 116, 2475  
Rieke, G.H., Lebofski, M.J., 1985, ApJ, 288, 618  
Stetson, P., 1993, User's Manual for DAOPHOT II

This figure "ivanovFig1.jpg" is available in "jpg" format from:

<http://arxiv.org/ps/astro-ph/0009374v1>

This figure "ivanovFig2.jpg" is available in "jpg" format from:

<http://arxiv.org/ps/astro-ph/0009374v1>